2009

The Cyclin-dependent Kinase Activator, Spy1A, Is Targeted for Degradation by the Ubiquitin Ligase NEDD4

Mohammad Al Sorkhy
University of Windsor

Ryan Craig
University of Windsor

Brenna Market
University of Windsor

Ryan Ard

Lisa A. Porter
University of Windsor

Protein Synthesis Post-translation Modification and Degradation:

The CDK activator, Spy1A, is targeted for degradation by the ubiquitin ligase Nedd4

Mohammad Al Sorkhy, Ryan Craig, Brenna Market, Ryan Ard and Lisa A. Porter

J. Biol. Chem. *published online December 3, 2008*

Access the most updated version of this article at doi: 10.1074/jbc.M804847200

JBC Papers in Press. Published on December 3, 2008 as Manuscript M804847200
The latest version is at http://www.jbc.org/cgi/doi/10.1074/jbc.M804847200

THE CDK ACTIVATOR, SPY1A, IS TARGETED FOR DEGRADATION BY THE UBIQUITIN LIGASE NEDD4*.

Mohammad Al Sorkhy[1], Ryan Craig[1], Brenna Market[2], Ryan Ard[1] and Lisa A. Porter[1]

[1] University of Windsor, Windsor, ON N9B 3P4;[2] University of Western Ontario, London, ON N6A 5C1

Running title: Nedd4 regulates Spy1A turnover.

* This work was supported by operating funds from a partnership between the Canadian Institutes of Health Research (CIHR) and the Canadian Breast Cancer Research Alliance (CBCRA) (#151092). M.A.S. acknowledges support from the University of Windsor, the Ontario Graduate Scholarship in Science and Technology (OGSST) and an NSERC PGD2, B.M. is supported by an NSERC CGSM and L.A.P. gratefully acknowledges support from the CIHR New Investigator Program.

‡Address correspondence to: LA Porter 401 Sunset Ave. Windsor, ON N9B3P4. (519) 253-3000 x4775,Fax: (519) 571-3609, Email:lporter@uwindsor.ca

Spy1A is a cyclin-like protein required for progression through G_1/S phase of the cell cycle. Elevated Spy1A protein levels have been implicated in tumorigenesis and are attributed to overriding the DNA damage response and enhancing cell proliferation. Understanding how Spy1A is produced and degraded is essential in resolving how it contributes to normal and abnormal growth processes. Herein, we demonstrate that Spy1A is degraded in a cell-cycle-dependent manner during mitosis via the ubiquitin-proteasome system. We have resolved the E3 ligase and essential phosphorylation sites mediating Spy1A degradation. Furthermore, we have determined that non-degradable forms of Spy1A do not trigger cell cycle arrest but rather contribute to uncontrolled cell growth. Further investigation into the regulation of Spy1A may reveal novel strategies for understanding the etiology and progression of specific growth disorders.

Members of the Speedy/RINGO family are unique cyclin-like regulators of the cell division cycle. There are now five members characterized in mammals exhibiting distinct tissue expression patterns and functional specificity (1). The originally characterized family member Spy1A1, herein referred to as Spy1A, is expressed constitutively in most human tissues; it shortens the G1/S transition through activation of CDK2 and is essential for cell proliferation to occur (2). Activation of CDKs by Spy1/RINGO proteins is thought to occur in an atypical fashion, independent of cyclin binding and in the absence of CDK phosphorylation within the T-loop (3). Spy1A can also act in a unique fashion to prevent inhibition of CDK2 by $p27^{Kip1}$ (p27), this occurs through direct interactions with the p27 protein and results in enhanced degradation of p27 (4,5). At a cellular level Spy1A also plays a role in the DNA damage response, functioning to enhance cell survival and promote cell proliferation in lieu of apoptosis (6,7). Our lab and others have demonstrated that Spy1A is capable of promoting precocious development and tumorigenesis in the mammary gland and that Spy1A protein levels are implicated in

invasive ductal carcinoma of the breast (8,9). Hence, determining how Spy1A protein levels are regulated may reveal novel information regarding the dynamics of cell cycle control during normal and abnormal growth conditions.

In mammals, Spy1A mRNA is known to be up-regulated during G_1/S; however regulation at the protein level has not been studied (2). The *Xenopus* homologue of Spy1A, X-Spy1, has been shown to undergo steps of proteasome dependent processing and degradation in a manner dependent on the initiation and progression of meiotic events (10). Degradation of X-Spy1 occurs following meiosis I and is mediated by the ubiquitin ligase Siah-2, this depends on phosphorylation of X-Spy1 on a carboxy terminal residue S243 (10). Cyclin proteins in general are tightly regulated temporally and spatially through the cell cycle, controlled on a fundamental level by the ubiquitin-proteasome system (UPS). The UPS is the primary mechanism involved in the selective degradation of intracellular and membrane-bound proteins, and aberrations in this critically important system are correlated to many diseases including cancer (11,12). Ubiquitination involves the conjugation of ubiquitin to a substrate protein via a concerted effort from three classes of enzymes: the ubiquitin-activating enzyme E1, the ubiquitin-conjugating enzyme E2, and the ubiquitin-protein ligase E3 (13). The E3 enzyme catalyzes the formation of a chain of ubiquitin molecules which then targets the substrate protein for degradation by the 26S proteasome (12,14,15). Given the functional cyclin-like properties of Spy1A it is a valid hypothesis that Spy1A may also be subject to a cell cycle dependent ubiquitin-mediated proteolysis, however whether the mammalian somatic cell cycle regulates this critical protein in the same manner as that seen during oocyte maturation in *Xenopus* warrants investigation.

Herein we demonstrate that Spy1A is ubiquitinated and degraded during G_2/M phase of the cell cycle. We have determined 3 key amino acids within the N-terminal region of Spy1A which are essential to support regulated degradation of the protein and we have demonstrated that the C-terminal region, known to regulate X-Spy1 degradation, is dispensable for degradation of the mammalian homologue. We have resolved that the E3 ligase Neuronal-Precursor-Cell-Expressed Developmentally Downregulated-4 (Nedd4) is capable of binding to Spy1A, and that dominant negative forms and knockdown of Nedd4 reduce ubiquitination and subsequent degradation of Spy1A. Furthermore, we show that non-degradable forms of Spy1A do not trigger intrinsic cell cycle checkpoints but rather promote cell proliferation; demonstration that this mechanism may contribute to tumorigenesis.

EXPERIMENTAL PROCEDURES

Cell Culture - Human mammary breast cancer cells, MCF7 (ATCC) and human embryonic kidney cells, HEK293 (293; ATCC), were maintained in DMEM medium (Sigma) containing 2mM L-glutamine (Sigma), penicillin and streptomycin (Invitrogen), and were cultured in a 5% CO_2 environment. MCF7 cells were supplemented with 10% (vol/vol) fetal calf serum (Sigma) and 293 cells were supplemented with 10% fetal bovine serum.

Plasmids and Mutagenesis - The Nedd4-PCEP plasmid (Nedd4), dominant negative Nedd4-PCEP plasmid ($Nedd4^{DN}$) and empty vector control (PCEP) were provided by Dr. Dale S. Haines (Temple University School of Medicine). HA-Ubiquitin (HA-Ub) was

provided by Dr. Sylvain Meloche (Université de Montréal). siRNA against Nedd4-1 was synthesized by inserting the oligo 5' GATGAAGCCACCATGTATA into the pSUPER-basic vector, as previously described (16). As a control, LacZ siRNA (siCntl) was synthesized and inserted into pSUPER-basic vector as described (21). Creation of Myc-Spy1A-PCS3 vector was described previously (2) . QuikChange Multi-Site-Directed Mutagenesis (SDM; Stratagene) was used to incorporate new silent sites into the original Spy1-pJT0013 vector (2) in order to facilitate the cloning of deletion mutants A (DMA), B (DMB), C (DMC), G (DMG) and Z (DMZ). A BglII site was inserted by altering nucleotide 256 from T to C using the primers #A043 5'-GACGATTTAATTCAAGATCTCTTG TGGATGGACTGCTGC-3' and #A044 5'-GCAGCAGTCCATCCACAAGAGAT CTTGAATTAAATCGTC-3' to construct the pRA01 vector. Using the pRA01 plasmid a Mlu site was also added by altering nucleotide 175 from C to G using #A004 5'-CAACAAATCTAAACGCGTCAAAG GACCTTGTCTGG-3' and #A005 5'-CCAGACAAGGTCCTTTGACGCGTT TAGATTTGTTG-3' to make the vector pRA02. The pRS2 vector was constructed from Spy1-pJT0013 by creating an NdeI site just after the stop codon using the primers #A045 5'-GTCTTGTGTCCATATGTGTTTTGTG GTGACCC-3' and #A046 5'-GGGTCACCACAAAACACATATGG ACACAAGAC-3'. The pRS1 vector was constructed by creating a MluI site in the Spy1-pJT0013 plasmid by altering nucleotide nucleotide 175 from C to G using primers #A004 5'-CAACAAATCTAAACGCGTCAAAG GACCTTGTCTGG-3' and #A005 5'-CCAGACAAGGTCCTTTGACGCGTTTA GATTTGTTG-3'. DMA was created by digesting wild-type Spy1A (in pRS1) with NdeI and MluI in order to remove the first 57 amino acids of the protein. DMB was created by digesting wild-type Spy1A (in pRA02) with MluI and BglII in order to remove 27 amino acids. DMC was created by digesting wild-type Spy1A (in pRA01) with BglII and NcoI in order to remove 61 amino acids. DMG was created by digesting wild-type Spy1A (in pJT0013) with NcoI and BbsI in order to remove 94 amino acids. Finally, DMZ was created by digesting wild-type Spy1A (in pRS1) with BbsI and NdeI in order to remove the last 47 amino acids. Gel electrophoresis of these digestions was run on a 1% agarose gel; the desired band was excised and gel-extracted (Bio Basics) for ligation using T4 DNA ligase (Fermentas). For all five deletion mutants, linkers containing a silent restriction site, PstI, and complementary sticky ends were designed, commercially synthesized (Sigma), annealed and utilized in the ligations. In each case, 20 µL ligation reactions were carried out at 22°C for 2-4 hrs. containing a 1:3 vector to linker ratio. Ligations were transformed into DH5α cells and selected for ampicillin resistance, mini-prepped, and digested with PstI (Fermentas) to detect the correct ligation. The five Spy1A deletion mutants (depicted in Fig. 3A), spanning the length of the gene, were moved from the pJT0013 into pCS3 using EcoRI and XbaI sites flanking the gene.

SDM was also carried out using the PCS3 vector to generate the Spy1A-T15A, Spy1A-T33A, Spy1A-S22A and Spy1A-S247A mutants. Spy1A-T15A was designed using the primers #A151 5'-GAGACACCACCTACTGTCGCTGTTTA TGTAAAATCAG-3' and #A152 5'-CTGATTTTACATAAACAGCGACAGTA GGTGGTGTCTC-3'; Spy1A-T33A was

designed using the primers #A-153 5'-CAGCCTAAAAAGCCCATTGCACTGAAGCGTCCTATTTG-3' and #A154 5'-CAAATAGGACGCTTCAGTGCAATGGGCTTTTTAGGCTG-3'; Spy1A-S22A was designed using the primers #A139 5'-GTTTATGTAAAATCAGGGGCCAATAGATCACATCAGC-3' and #A140 5'-CTGATGTGATCTATTGGCCCCTGATTTTACATAAAC-3; Spy1A-S247A was designed using the primers #A143 5'-GGATTGTCTTCATCATCAGCGTTATCCAGTCATACTGCAGGGGTG-3' and #A144 5'-CACCCCTGCAGTATGACTGGATAACGCTGATGATGAAGACAATCC-3'. Successful cloning in all cases was determined by DNA sequencing (Robarts Sequencing Facility; Univ. of Western Ontario).

Inhibitors and Antibodies - The following antibodies were used: Spy1A (NB 100-2521; Novus), Nedd4 (ab14592; Abcam), Myc (9E10 and C19; Santa Cruz), HA (Y11 and F7; Santa Cruz), Actin (MAB1501R; Chemicon), Cyclin E (551157; BD Pharmingen), IgG (SC66186; Santa Cruz). The following inhibitors were used: N-Acetyl-L-leucyl-L-leucyl-L-norleucinal N-Acetyl-Leu-Leu-Norleu-al (LLNL; Sigma A6060); MG132 (Sigma C2211); Cyclohexamide (Sigma C7698); nocodazole (Sigma M1404) , thymidine (Sigma T1895) and Lactacystin (Boston Biochem I-116).

Transfections - Calcium phosphate precipitation transfections were carried using 10-12 µg of DNA per 10 cm tissue culture plate. 250 µL $CaCl_2$ was incubated with the DNA for 30 sec., 250µL 2x BBS at pH 7.01 was added while vortexing and the solution was incubated for 10 min. The mixture was added slowly to the cells and then incubated in 3% CO_2 for 12-16 hrs. Media was then changed and plates were returned to 5% CO_2 for at least 12 hrs. prior to harvest.

Cell Synchronization and Flow Cytometry - 293 cells were synchronized using double thymidine block. Briefly, cells were cultured in media containing 2 mM thymidine for 16 hrs., followed by release into normal media for 8 hrs. and then a second thymidine block for 14 hrs., and then released into media containing 70 ng/ml nocodazole (with or without 10 µM MG132 as indicated). MCF7 cells were synchronized by being cultured in a serum-free media for 48 hrs. followed by release into media containing serum and 70 ng/ml nocodazole. 293 and MCF7 cells were trypsinized at specified times, washed twice in PBS, and then either used immediately or fixed and stored at -20°C. Fixation was carried out by resuspending cells at 2 x 10^6 cells in 1 mL of PBS, followed by slow addition of an equal amount of 100% ethanol. Within 1 week, fixed cells were pelleted, washed, and resuspended in 300 µL of PBS. Samples were then prepared for flow cytometry by treating with 1 µL of 10 mg/mL stock of DNase free RNase (Sigma) and 50 µL of 500 mg/mL propidium iodide stock solution. Data was collected using a Beckman Coulter FC500 (Biology Dept.; U of Windsor) and cell cycle profiles were analyzed using CPX Beckman Coulter FC500 software.

Immunoblotting - Cells were lysed in 0.1% NP-40 lysis buffer (0.1% NP-40, 1M Tris pH 7.5, 0.5M EDTA, 5M NaCl) containing protease inhibitors (PMSF 100 µg/mL, aprotinin 5µg/mL, leupeptin 2µg/mL) for 30 min on ice. Bradford Reagent was used to determine the protein concentration following the manufacturer's instructions (Sigma). Aliquots of lysates containing 20-30 µg protein were subjected

to electrophoresis on denaturing 10-12% SDS polyacrylamide gels and transferred to Polyvinylidene Fluoride-Plus transfer membranes (Osmonics Inc.) for 2 hrs. at 30V using a wet transfer method. Blots were blocked for 2 hrs. in TBST containing 3% non-fat dry milk (blocker) at room temperature. Primary antibodies were reconstituted in blocker and incubated over night at 4°C at a 1:1000 dilution for all antibodies, and secondary antibodies were used at a 1:10,000 dilution in blocker for 1 hr at room temperature. Blots were washed three times with TBST following incubation with both the primary and secondary antibodies. Washes were 6 min each following the primary antibody and 10 min each following the secondary antibody. Chemilumiminescent Peroxidase Substrate was used for visualization following the manufacturer's instructions (Pierce). Chemiluminescence was quantified on an Alpha Innotech HD2 (Fisher) using AlphaEase FC software.

Immunoprecipitation reactions were carried out using equal amounts of protein (~200µg/mL) incubated with 2 µg of primary antisera, as indicated, overnight at 4°C. This was followed by the addition of protein A–Sepharose (Sigma) and incubated at 4°C with gentle rotation for an additional 2 hrs. Complexes were washed extensively with 0.1% NP-40 lysis buffer and resolved by 10% SDS-PAGE.

In Vivo Labeling - 293 cells were treated with 10µM MG132 and 70 ng/ml nocadozol for 14 hrs. followed by incubation in phosphate-free media for 2 hrs. and cells were labeled with [^{32}P]orthophosphate (0.3 mCi/ml) (PerkinElmer) for 4 h at 37°C. Cells were lysed and immunoprecipitated with Myc antisera. Immunoprecipitations were washed rigorously with TBST and samples were analyzed by 10% SDS page gel. Gels transferred to PVDF membranes were visualized using a Cyclone phosphoimager and quantified using OptiQuant software (Perkin Elmer; Biology Dept.; U of Windsor).

In Vivo Ubiquitination Assays - 293 cells were plated and transfected appropriately in a 100-mm dish. 24 hrs. after transfection cells were treated with 10 µM MG132 for 14 hrs. Cells were then collected, pelleted by centrifugation, lysed in 200 µl of preboiled lysis buffer [50 mM Tris-HCl (pH 7.5), 0.5 mM EDTA, 1% SDS, and 1 mM DTT], and further boiled for an additional 10 min. Lysates were clarified by centrifugation at 13,000 rpm on a microcentrifuge for 10 min. Supernatant was diluted 10 times with 0.5% NP40 buffer and immunoprecipitated with anti-Myc antibody. Immunoprecipitates were washed 3 times and resolved by 10% SDS-PAGE, followed by immunoblotting with anti-HA antibody.

RESULTS

Spy1A protein levels are regulated in a cell cycle dependent fashion. MCF7 and 293 cells were blocked in G_1 using serum starvation and thymidine block procedures respectively. Cells were released into serum and nocodozole containing media and populations enriched in G1 or G_2/M phases of the cell cycle were collected as determined by flow cytometry analysis (Fig. 1A and C). Cell lysates from the respective populations were immunoblotted for endogenous Spy1A expression (Fig. 1B & D; upper panels). Cyclin E was utilized as a control for the cell cycle stage (Fig. 1B; middle panel), and Actin was used as the loading control (Fig. 1B and D; lower panels). These data demonstrate that Spy1A protein levels are greatly decreased during G_2/M phase of the cell cycle and support

that, like many important cell cycle proteins, Spy1A is tightly regulated in a cell cycle dependent fashion.

Spy1A degradation depends on phosphorylation within the N-terminal region. Using a panel of Spy1A deletion mutants (Fig. 2A), we began to narrow down the region within the Spy1A protein that was necessary for degradation. We first determined whether deletion of any of the regions of Spy1A would result in stabilization of the protein. 293 cells were transfected with wild-type Spy1A or deleted versions of the Spy1A protein, DMA-DMZ. Cells were synchronized at G_2/M and levels of Spy1A were monitored by immunoblotting (Fig. 2B; upper left panel). All deletion mutants of Spy1A were degraded by G_2/M phase with the exception of the mutant lacking the first 57 amino acids (DMA). Asynchronous cells demonstrate that all deletion mutants were expressed (Fig. 2B; upper right panel). Collectively, these data demonstrate that the N-terminal region of Spy1A is essential to mediate degradation of the protein and that unlike the *Xenopus* homolog of Spy1 the C-terminal region is dispensable for degradation.

Phosphorylation is often the key event regulating recognition of the substrate protein by the E3 (11). To determine whether deletion of the N-terminal region of Spy1A altered the phosphorylation status of the protein, orthophosphate labeling was performed on G2 populations of cells expressing either wild-type or Spy1A deleted of its N-terminal region (DMA) in the presence of MG132. Over 3 experiments a significant decrease in the incorporation of orthophosphate was repeatedly observed when the N-terminal region of Spy1A was deleted (Fig. 2C). From this information, we conclude that there is at least one phosphorylation site present within the N-terminal region of Spy1A that may play a significant role in regulating Spy1A stability.

Spy1A steady state levels are proteasome dependent. After determining the timing of Spy1A degradation during cell cycle progression, we set out to investigate the mechanism by which this occurs. To determine whether this mechanism was proteasome dependent we studied 293 cells in the presence or absence of the proteasome inhibitors MG132, Lactacystin and the calpain inhibitor LLNL. Spy1A protein levels were significantly elevated in the presence of MG132 as well as Lactacystin but not in the presence of the calpain inhibitor or the vehicle controls (Fig. 3A; upper panel; ETOH – vehicle for LLNL, DMSO – vehicle for MG132 and Lactacystin). This data implicates that Spy1A abundance is proteasome dependent. 293 cells were then utilized for an *in vivo* ubiquitination assay where cells were transiently transfected with HA-tagged ubiquitin (HA-Ub) and Myc-tagged Spy1A (Myc-Spy1A) in the presence of MG132 followed by immunoprecipitation with α-Myc (Fig. 3B; lower panel). Immunoblotting with α-HA revealed that Spy1A was labeled with HA-ubiquitin *in vivo* (Fig. 3B; upper panel). The experiment was then repeated using endogenous Spy1A and immunoprecipitation with α-HA. Immunoblotting with α-Spy1A revealed that Spy1A was indeed labeled with HA-ubiquitin *in vivo* (Fig. 3C; upper panel). Collectively these results demonstrate that Spy1 protein levels are regulated via the UPS. To determine whether the stability shown by DMA is due to lack of ubiquitination 293 cells were utilized in an *in vivo* ubiquitination assay. Cells were transiently transfected with HA-tagged

Ubiquitin (HA-Ub) and either Myc-tagged Spy1A (Myc-Spy1A), DMA or DMB in the presence of MG132 followed by immunoprecipitation with α-Myc (Fig 3D; lower panel) Immunoblotting with α-HA revealed that Spy1A and TMB were labeled with HA-ubiquitin *in vivo*, whereas TMA was not. This result demonstrates that lack of ubiquitination is responsible for the stability of the N-terminal deletion of Spy1A.

The E3 ligase Nedd4 regulates Spy1A degradation. There are many different E3 ubiquitin ligase enzymes that are able to function in the ubiquitination pathway. To determine which E3 ligase functions in the degradation of Spy1A a protein blast for the N-terminal region of Spy1A revealed a weak potential interaction region for WW domain containing proteins, PPxxxxY spanning from P11-Y17 in the Spy1A sequence. Immunoprecipitation with endogenous Spy1A followed by coomassie staining revealed a predominant band enriched in G2 populations of cells at approximately 110-115 kD (data not shown). It is known that the 114 kD WW domain-containing ligase Nedd4 (product of neuronal precursor cell-expressed developmentally down-regulated gene 4), while preferring the canonical PPxY sequence, also binds to a variety of proline rich regions with phosphorylated threonine or serine residues to trigger ubiquitination and subsequent degradation (15,17,18). Due to this we investigated the potential role of Nedd4 in Spy1A degradation. Interestingly, Nedd4 is a family of conserved E3 ubiquitin ligases found to function as both proto-oncogenes as well as tumor suppressors. Nedd4 is known to both mono-, di- and poly-ubiquitinate its target proteins, where polyubiquitinated proteins are selectively targeted for degradation by the proteosome (19). Clarifying the biology of the Nedd4 family and relevant substrates may provide important information for tumorigenesis (19-23). Co-immunoprecipitation of lysates overexpressing exogenous Nedd4 as well as Myc-Spy1A in the presence of MG132 demonstrates that Nedd4 interacts with Spy1A *in vivo* (Fig. 4A). These results were then confirmed by using endogenous binding in two different cell lines 293 and NIH3T3 (Fig. 4B). To further investigate whether Nedd4 is functioning as an ubiquitin ligase for Spy1A, we repeated the co-immunoprecipitation experiment using overexpression of wild-type Nedd4 or dominant negative Nedd4 ($Nedd4^{DN}$) in the presence of HA-Ub and MG132. $Nedd4^{DN}$ contains a single amino acid substitution which prevents the formation of a thioester bond with ubiquitin and hence renders Nedd4 inactive (12,14,15). Immunoblotting for Spy1A, followed by quantification, revealed that HA-Ub incorporation was significantly decreased in the presence of $Nedd4^{DN}$ (Fig. 4C). To further establish whether Nedd4-1 was required for both binding and degradation of Spy1A, 293 cells were transfected with either siNedd4 or an siRNA control (siLacZ; siCntl) followed by immunoblotting with α-Nedd4 (Fig. 4D upper panel), α-Spy1A (Fig. 4D Middle Panel) and α-actin (Fig. 4D lower panel). Densitometry of detected bands over 3 separate experiments demonstrate that Spy1A protein levels are accumulating when Nedd4 levels are reduced with siRNA. To examine the effect of knockdown of Nedd4-1 on Spy1A-Nedd4 binding 293 lysates overexpressing Myc-Spy1A and either siNedd4 or siCntl were immunoprecipitated with α-Myc (Fig. 4E left panels). Immunoblotting with α-Nedd4 shows that Nedd4-Spy1 binding was significantly

reduced following knockdown of Nedd4-1 (Fig. 4E upper panel). To assess the effect of Nedd4 on endogenous Spy1A, Nedd4 was transfected into 293 cells in the presence and absence of MG132, and endogenous levels of Spy1A were measured. Overall Spy1A protein levels were consistently decreased in 2 separate experiments by at least 20% when Nedd4 was transiently transfected in the absence of MG132 as compared to when MG132 was present (Fig. 4F). To confirm the effect of $Nedd4^{DN}$ and siNedd4 on Spy1 protein stability, $Nedd4^{DN}$ or siNedd4wt- Nedd4 and Myc-Spy1A were transfected into 293 cells. 12 hrs. post-transfection cells were released, at 16 hrs post-transfection 50 μg/ml cycloheximide was added to prevent *de novo* protein synthesis. Over 3 separate experiments immonoblotting for Spy1A, followed by quantification, showed that wtSpy1 had a half life of approximately 1 hr. and that stability was decreased significantly in the presence of Nedd4 but was significantly more stable in the cells transfected with $Nedd4^{DN}$ and siNedd4 (Fig. 4G and 4H). Collectively, this data demonstrates a novel relationship between two proteins previously implicated in tumorigenesis; Spy1A and Nedd4.

Residues T15, S22, and T33 are essential for Spy1A degradation. Cell cycle regulatory proteins which are targeted to the UPS rely on signal transduction mechanisms to control the timing of this essential event. We have demonstrated that the N-terminal region of Spy1A is essential for mediating degradation. Hence, we focused on elucidating sites within this region that may target the protein for degradation. Utilizing the NetPhos 2.0 Server tool residues T15, S22, and T33 were isolated as potential phosphorylation sites (24). Site-directed mutagenesis was performed to alter Spy1A residues T15, S22, and T33 to non-phosphorylatable alanines. Additionally we generated a similar mutation at S247 in the C-terminal region to serve as a control. 293 cells were transfected with the relevant constructs prior to synchronization at G_2/M. Surprisingly, mutation of all of T15, S22, and T33 to a non-phosphorylatable alanine prevented degradation and ubiquitination of Spy1A (Figs. 5A & B). Blotting asynchronous cell populations revealed that protein expression was not affected (Fig. 5A; right panel) and flow cytometry analysis demonstrated that effects at T15, S22 and T33 were not due to a failure of the mutant Spy1 expressing cells to properly arrest in G2 phase (Fig. 5E; upper panel). This suggests that phosphorylation, or maintenance of charge of all three of T15, S22, and T33 is essential in regulating the turnover of Spy1A. To further assess the effect of these mutations on Spy1A degradation, 293 cells were transfected and then treated with 50 μg/ml cyclohexamide 16hrs. post-transfection. Immunoblotting for Spy1A showed that cells transfected with the mutants have stabilized Spy1A levels (Fig. 5C). Quantifying 3 separate experiments demonstrate that indeed all 3 mutations significantly enhance the stability of Spy1A protein (Fig. 5C; right hand panel). To assess whether these sites are phosphorylated *in vivo* a triple mutant (Spy1A-TST) was created where all 3 elucidated sites were mutated to a nonphosphorylatable alanine (T15A, S22A and T33A). Phosphorylation of Spy1A-TST at G2/M was compared to that of wt-Spy1A using an orthophosphate labeling experiment. A significant decrease in phosphorylation was observed with the triple mutant (Fig. 5D), demonstrating that Spy1A is phosphorylated at residues T15, S22 and T33 during G2 phase of the cell

cycle. Importantly, these mutations provide us with a valuable tool to assess the essentiality of Spy1A degradation on cell cycle dynamics.

Aberrant Spy1A degradation enhances cell proliferation but does not trigger a cell cycle arrest. Cyclin protein levels serve as a monitoring mechanism for the cell to ensure that each phase of the cell cycle is complete before the next is initiated; such checkpoint mechanisms are essential in protecting the integrity of the cell. The Spy1/RINGO family members have been functionally characterized as novel cyclin-like proteins; hence we utilized the Spy1 degradation mutants in order to determine whether progression of the somatic cell cycle requires the timely degradation of Spy1A. Cells from figure 5A which were overexpressing Spy1-wt, Spy1-T15A, Spy1-T33A, Spy1-S22A or Spy1-S247A were analyzed via flow cytometry analysis (Fig. 5E). Wild-type and mutant Spy1A constructs revealed very similar cell cycle profiles (Fig. 5E asynchronous cells; lower panel), demonstrating that prevention of Spy1A degradation in this cell type does not trigger a cell cycle arrest.

To test the effects of ablating Spy1A degradation on cell proliferation live and dead cell populations were monitored by trypan blue analysis. Spy1A and mutant constructs significantly enhance cell proliferation as compared to mock with p values of 0.01 for mock:WT, 0.001 for mock:Spy1A-T15A, 0.0004 for mock:Spy1A-T33A, and 0.001 for mock:Spy1A-S22A (these stats are not reflected in Fig. 5F). There was no statistical change in the number of dead cells from one transfection to another (Fig. 5F; grey bars). Interestingly, Spy1 degradation mutants statistically enhanced proliferation over Spy1A alone by 20-60% (Fig. 5F; black columns). p-values for these comparisons were 0.009 for WT:Spy1A-T15A, 0.002 for WT:Spy1A-T33A and 0.03 for WT:Spy1A-S22A.

Collectively, these data demonstrate that residues T15, S22, and T33 within the N-terminal region of Spy1A are important phosphorylation sites for mediating the degradation of the protein. Furthermore, preventing degradation of Spy1A does not trigger cell cycle arrest but rather results in enhanced cell proliferation; hence representing a mechanism which may contribute to tumorigenesis.

DISCUSSION

Importance of Spy1A degradation in cell cycle regulation. Tight regulation over the protein levels of cyclins and activity of their respective kinase is known to be one mechanism by which the cell ensures the proper timing of cell cycle events (25). More recently it has come to light that CDKs can also be activated by members of the Speedy/RINGO family. These proteins lack any sequence homology with cyclins however our data demonstrates that, like the cyclins, Spy1A is tightly regulated at the protein level through the cell cycle. The importance of Speedy/RINGO proteins in the cell cycle is irrefutable, expression of Spy1A is essential for cells to progress through DNA synthesis, overexpression enhances cell proliferation and deregulated levels lead to aberrant growth (5,8) (9). In immortalized cells our results demonstrate that non-degradable mutants of Spy1A do not trigger a cell cycle arrest but rather promote significantly enhanced proliferation over Spy1 wild-type expression alone. Whether preventing degradation results in Spy1 activation of unique CDKs, and whether this contributes toward the proliferative phenotype of these mutants

remains to be determined. Most importantly, these data support the possibility that altered degradation of the Spy1A protein is an unchecked cell cycle event which contributes toward proliferation and may play a mechanistic role in human tumorigenesis.

The Spy1A degradation mechanism. Herein, we demonstrate a novel interaction between Spy1A and the E3 ligase Nedd4 which mediates the degradation of Spy1A. This demonstrates that in addition to functional differences, the mammalian Spy1A isoform is subject to differential protein regulation as compared to its *Xenopus* counterpart (10). The domain structure of Nedd4 family members are very similar and contain a series of typically two to four WW domains which function as recognition sites for specific substrates or adaptor proteins (26,27). The WW domains of Nedd4 preferentially recognize PPxY motifs in their substrates (28). The N-terminal region of Spy1A lacks this consensus site; however is known that Nedd4 can also interact with phosphorylated threonine or serine residues to trigger ubiquitination and subsequent degradation (15) (18). Notably all deletion mutant constructs for Spy1A, depicted in figure 2A, were found to interact with Nedd4 *in vivo* (data not shown). This suggests that the Nedd4-Spy1A interaction relies on at least 2 separate binding regions in the Spy1A protein; resolution of these required binding regions remain to be determined. Following mutagenesis of 3 potential phosphorylation sites within the N-terminal region of Spy1A, we have determined that preservation of amino acids 15-33 is generally important for Spy1A degradation. T15 is completely conserved among the mammalian Spy1A homologues, and is preceded by a highly conserved proline rich region (PPTV); whether these sites are involved in proteolysis of other Spy1/RINGO family members remains to be determined. Furthermore, the Nedd4 family consists of nine members, all containing WW domains. We know from overexpression assays using Nedd4-1 cDNA that this member of the Nedd4 family is capable of interacting and promoting the ubiquitination and degradation of Spy1A. Additionally, specific knockdown of Nedd4-1 prevented the degradation of Spy1 and interactions between Spy1-Nedd-4, collectively these data strongly support that Nedd4-1 is the specific isoform mediating Spy1 degradation. Whether other members of the Nedd4 family are also capable of regulating the degradation of Spy1A is currently not known. It is known that the Nedd4 family are capable of also mono- and di-ubiquitinating their substrate proteins. While we cannot rule out that these modifications also occur, our data demonstrate that Spy1A can be polyubiquitinated by Nedd4 and that this targets the protein for degradation.

Spy1A-Nedd4 interaction in cancer. From the current catalogue of known Nedd4 substrates it appears that Nedd4 can act as both a proto-oncogene, as well as a tumor suppressor under different circumstances. For example, Nedd4 has been shown to mediate the degradation of the vascular endothelial growth factor receptor 2 (VEGF-R2) (20). VEGF-R2 is a positive regulator of cell proliferation, migration, and angiogenesis (29), and it is known to be up-regulated in colon (30), brain (31), and breast cancer (32). In addition, Nedd4 has been shown to lead to the down-regulation of the insulin-like growth factor 1 receptor (IGF-1R) (21), which has been implicated in both the initiation and development of many human cancers types (33). Our data provides further evidence that Nedd4 can function

like a tumor suppressor to regulate the levels of proteins stimulating cell growth mechanisms. Conversely, Nedd4, or Nedd4 family members, have been shown to regulate the degradation and function of important tumor suppressor genes such as the phosphatase and tensin homolog 1 (PTEN), p53 and the p53 family member, p73 (19,22,23). This novel interaction between the Spy1/RINGO family and Nedd4 strengthens the possibility that Nedd4 substrate specificity may contribute to oncogenesis, thereby allowing for the accumulation of proliferative proteins such as Spy1A. Further resolving how this mechanism is functioning in human cancers is an important direction that may provide a novel direction in the design of cancer therapeutics.

Acknowledgments - We thank Drs. D.S. Haines and D. Rotin for providing us with plasmids for this study. Our gratitude to Drs. P. Vacratsis, M. Crawford and S. Anavoranich for valuable advice and to Ms. J. Ritchie and D. Myers for help on this manuscript.

REFERENCES

1. Cheng, A., Xiong, W., Ferrell, J. E., Jr., and Solomon, M. J. (2005) *Cell Cycle* **4**(1), 155-165
2. Porter, L. A., Dellinger, R. W., Tynan, J. A., Barnes, E. A., Kong, M., Lenormand, J. L., and Donoghue, D. J. (2002) *J Cell Biol* **157**(3), 357-366
3. Karaiskou, A., Perez, L. H., Ferby, I., Ozon, R., Jessus, C., and Nebreda, A. R. (2001) *J Biol Chem* **276**(38), 36028-36034
4. Porter, L. A., Kong, M., and Donoghue, D. J. (2003) *Mol Biol Cell* **14**, 3664-3674
5. McAndrew, C. W., Gastwirt, R. F., Meyer, A. N., Porter, L. A., and Donoghue, D. J. (2007) *Cell Cycle* **6**(15), 1937-1945
6. Barnes, E. A., Porter, L. A., Lenormand, J. L., Dellinger, R. W., and Donoghue, D. J. (2003) *Cancer Res* **63**(13), 3701-3707
7. Gastwirt, R. F., Slavin, D. A., McAndrew, C. W., and Donoghue, D. J. (2006) *J Biol Chem*
8. Zucchi, I., Mento, E., Kuznetsov, V. A., Scotti, M., Valsecchi, V., Simionati, B., Vicinanza, E., Valle, G., Pilotti, S., Reinbold, R., Vezzoni, P., Albertini, A., and Dulbecco, R. (2004) *Proc Natl Acad Sci U S A* **101**(52), 18147-18152
9. Golipour, A., Myers, D., Seagroves, T., Murphy, D., Evan, G. I., Donoghue, D. J., Moorehead, R. A., and Porter, L. A. (2008) *Cancer Res* **68**(10), 3591-3600
10. Gutierrez, G. J., Vogtlin, A., Castro, A., Ferby, I., Salvagiotto, G., Ronai, Z., Lorca, T., and Nebreda, A. R. (2006) *Nat Cell Biol* **8**(10), 1084-1094
11. Chen, C., Seth, A. K., and Aplin, A. E. (2006) *Mol Cancer Res* **4**(10), 695-707
12. Robinson, P. A., and Ardley, H. C. (2004) *J Cell Sci* **117**(Pt 22), 5191-5194
13. Hershko, A., and Ciechanover, A. (1992) *Annu Rev Biochem* **61**, 761-807
14. Hershko, A., and Ciechanover, A. (1998) *Annu Rev Biochem* **67**, 425-479
15. Shearwin-Whyatt, L., Dalton, H. E., Foot, N., and Kumar, S. (2006) *Bioessays* **28**(6), 617-628
16. Pak, Y., Glowacka, W. K., Bruce, M. C., Pham, N., and Rotin, D. (2006) *J Cell Biol* **175**(4), 631-645
17. Harvey, K. F., and Kumar, S. (1999) *Trends Cell Biol* **9**(5), 166-169

18. Sutterluty, H., Chatelain, E., Marti, A., Wirbelauer, C., Senften, M., Muller, U., and Krek, W. (1999) *Nat Cell Biol* **1**(4), 207-214
19. Wang, X., Trotman, L. C., Koppie, T., Alimonti, A., Chen, Z., Gao, Z., Wang, J., Erdjument-Bromage, H., Tempst, P., Cordon-Cardo, C., Pandolfi, P. P., and Jiang, X. (2007) *Cell* **128**(1), 129-139
20. Murdaca, J., Treins, C., Monthouel-Kartmann, M. N., Pontier-Bres, R., Kumar, S., Van Obberghen, E., and Giorgetti-Peraldi, S. (2004) *J Biol Chem* **279**(25), 26754-26761
21. Vecchione, A., Marchese, A., Henry, P., Rotin, D., and Morrione, A. (2003) *Mol Cell Biol* **23**(9), 3363-3372
22. Laine, A., and Ronai, Z. (2007) *Oncogene* **26**(10), 1477-1483
23. Rossi, M., De Laurenzi, V., Munarriz, E., Green, D. R., Liu, Y. C., Vousden, K. H., Cesareni, G., and Melino, G. (2005) *Embo J* **24**(4), 836-848
24. Blom, N., Gammeltoft, S., and Brunak, S. (1999) *J Mol Biol* **294**(5), 1351-1362
25. Nurse, P. M. (2002) *Biosci Rep* **22**(5-6), 487-499
26. Anan, T., Nagata, Y., Koga, H., Honda, Y., Yabuki, N., Miyamoto, C., Kuwano, A., Matsuda, I., Endo, F., Saya, H., and Nakao, M. (1998) *Genes Cells* **3**(11), 751-763
27. Ingham, R. J., Gish, G., and Pawson, T. (2004) *Oncogene* **23**(11), 1972-1984
28. Murillas, R., Simms, K. S., Hatakeyama, S., Weissman, A. M., and Kuehn, M. R. (2002) *J Biol Chem* **277**(4), 2897-2907
29. Ferrara, N. (2005) *Oncology* **69 Suppl 3**, 11-16
30. Giatromanolaki, A., Koukourakis, M. I., Sivridis, E., Chlouverakis, G., Vourvouhaki, E., Turley, H., Harris, A. L., and Gatter, K. C. (2007) *Eur J Clin Invest*
31. Puputti, M., Tynninen, O., Sihto, H., Blom, T., Maenpaa, H., Isola, J., Paetau, A., Joensuu, H., and Nupponen, N. N. (2006) *Mol Cancer Res* **4**(12), 927-934
32. Ryden, L., Linderholm, B., Nielsen, N. H., Emdin, S., Jonsson, P. E., and Landberg, G. (2003) *Breast Cancer Res Treat* **82**(3), 147-154
33. Miller, B. S., and Yee, D. (2005) *Cancer Res* **65**(22), 10123-10127

FIGURE LEGENDS

FIGURE 1. **Spy1A protein levels are regulated in a cell cycle dependent fashion.** (A) Left panel; Flow cytometry profiles for MCF7 cells either untreated (Cntl), collected immediately following release from serum starvation (G1) or collected 16 hrs. following release into nocodozole containing media. Right panel; Percentage of cells in each phase of the cell cycle as determined by flow cytometry analysis software. (B) Cell lysates from each population described in A were immunoblotted with α-Spy1A, α-Cyclin E and α-Actin. (C) Left panel; Flow cytometry profiles for 293 cells either untreated (Cntl), blocked by double thymidine block (G1) or blocked and then released into media containing serum and nocodazole (G2). Right panel; Percentage of cells in each phase of the cell cycle as determined by flow cytometry analysis software. (D) Cell lysates from each population described in C were immunoblotted with α-Spy1A and α-Actin.

FIGURE 2. **Spy1A degradation relies on the N-terminal region.** (A) A schematic diagram for the different Spy1A deletion mutants is depicted and restriction sites used for cleavage of the region are indicated. (B) 293 cells were transfected with Myc-Spy1A-PCS3 (wt) or the different deletion mutant DMA-DMZ (A-Z). Transfected cells were treated with nocodazole (left hand panels; synchronous) or no treatment (right hand panels; asynchronous) for 16 hrs. post transfection. Lysates were immunoblotted with α-Myc or α-Actin. (C) 293 cells were transfected with Myc-Spy1A-PCS3 (wt) or deletion mutant A (DMA). 12 hrs post-transfection cells were treated with nocodazole and MG132 for 14 hrs. followed by orthophosphoric acid ^{32}P for an additional 4 hrs. Cells were lysed, immunoprecipitated with α-Myc and imaged on a Cyclone phosphorimager (upper blot; left panel). Immunoblot for α-Myc was used as a control (lower blot). Incorporation of ortho-phosphate was quantified using OptiQuant software, right panel represents results over 3 separate experiments. Error bars reflect SEM. T-test was performed, ** $p \leq 0.01$.

FIGURE 3. **Spy1A steady state levels are proteosome dependent.** (A) Cells were treated for 14 hrs with a calpain inhibitor (LLNL; 25μM) or proteasome inhibitors (MG132; 10μM and Lactacystin; 10μM) as well as the relevant vehicle control for LLNL (ETOH) and MG132 and lactacystin (DMSO). Lysates were analyzed by immunoblotting with α-Spy1A and α-Actin. (B) 293 cells were transfected with HA ubiquitin (HA-Ub), Myc-Spy1A-PCS3 (Myc-Spy1A) and PCS3 empty vector (Myc-Cntl), 12 hr. post-transfection 10μM MG132 was added for 14hr. α-Myc immunoprecipitations were immunoblotted with α-HA and α-Myc. (C). 293 cells were transfected with HA Ubiquitin (HA-Ub), or empty vector control (PMT123), 12 hr. post-transfection 10μM MG132 was added for 14hr. α-HA immunoprecipitations were immunoblotted with α-Spy1A and α-IgG-mouse. (D) 293 cells were transfected with HA ubiquitin (HA-Ub), Myc-Spy1A, PCS3 empty vector, PMT123 empty vector, Spy1A-deletion mutant A (DMA) and Spy1A deletion mutant B (DMB) 12 hr. post-transfection 10μM MG132 was added for 14hr. α-Myc immunoprecipitations were immunoblotted with α-HA and α-Myc

FIGURE 4. **The E3 ligase Nedd4 regulates degradation of Spy1A.** (A) 293 cells were transfected with empty vectors (PCS3 or PCEP), Nedd4-PCEP (Nedd4) or Myc-Spy1A-PCS3 (Myc-Spy1A) and treated with MG132 for 14 hrs prior to harvest. α-Myc immunoprecipitations were immunoblotted with α-Nedd4 (upper panel) and α-Myc (lower panel). Lysates from NIH3T3 cells served as positive control for Nedd4 expression (+; lane 5). (B) 293 and NIH3T3 cells were treated with 10μM MG132 for 14 hr., lysates were immunoprecipitated with α-Nedd4 or α-IgG and immunoblotted with α-Spy1A (upper panel) or α-IgG (lower panel). (C) 293 cells were transfected with empty vectors (PMT123 or PCEP), Nedd4-PCEP (Nedd4), HA Ub-PMT123 (HA-Ub) or Nedd4-PCEP Dominant Negative ($Nedd4^{DN}$) and treated with MG132 for 14 hrs. prior to harvest. α-HA immunoprecipitations were analyzed by immunoblotting for α-Spy1A (upper panel) and α-HA (middle panel). Lysates were used to demonstrate Nedd4/$Nedd4^{DN}$ transfection (lower blot). Densitometry of Ha-Ub-Spy1A was performed and equalized using α-HA blot (right hand panel). This is one representative experiment of 3. (D) 293 cells were transfected with siRNA against Nedd4 (siNedd4) or siRNA against LacZ (siCntl). Lysates were immunoblotted with α-Nedd4 (upper blot), α-Spy1A (middle blot) and α-Actin (lower blot). Densitometry of Spy1 levels equalized to the Actin loading control over 3 separate experiments was performed (right hand panel). Error bars represent SEM. p-value for siCntl:siNedd4 = 0.001. (E) 293 cells were cotransfected with Myc-Spy1A and either siNedd4 or siCntl, 12 hr. post-transfection 10μM MG132 was added for 14hr. α-Myc immunoprecipitations (left hand panels) and lysates (right hand panels) were immunoblotted with α- Nedd4 (upper panel) or for α-Myc (lower panel). (F) 293 cells were transfected with PCEP empty vector control (lane 1) and Nedd4-PCEP (Nedd4; lanes 2 & 3). Cells were either treated with MG132 (lane 2) or DMSO (lanes 1 & 3). Lysates were immunoblotted with α-Spy1A and α-Actin. Densitometry for Spy1A levels was carried out and is depicted after equalization with Actin levels over 3 separate experiments (right hand panel). Error bars represent SEM. statistics reflect Nedd4 + or – MG132 as compared to control. **= $p<0.01$. (G) 293 cells were transfected with Myc-Spy1A-PCS3 (Myc-Spy1A) along with either PCEP empty vector (Cntl), Nedd4-PCEP (Nedd4) and, Nedd4-PCEP Dominant Negative ($Nedd4^{DN}$). 16 hrs. after transfection cyclohexamide was added and cells were collected at 30, 75 and 120 min. time points. Cell lysates were analyzed by immunoblotting for α-myc antibody. Actin was used as a loading control (lower panel). (H) 293 cells were transfected with Myc-Spy1A-PCS3 (Myc-Spy1A) along with either sicontrol (Cntl), Nedd4-PCEP (Nedd4) and, siNedd4. 16 hrs. after transfection cyclohexamide was added and cells were collected at 30, 75 and 120 min. time points. Cell lysates were analyzed by immunoblotting for α-myc antibody. Actin was used as a loading control (lower panel) (G & H) Lower panels represent densitometry where Spy1A expression is equalized with actin over 3 separate experiments. Error bars represent SEM. Statistics reflect Nedd4, $Nedd4^{DN}$ or siNedd4 transfections as compared with Cntl transfections at each time point. *= $p<0.05$, ** = $p<0.01$

FIGURE 5. **Phosphorylation on T15, T33 and S22 is needed for Spy1A degradation.** 293 cells were transfected with Spy1A wild-type (wt), Spy1A-T15A (T15A), Spy1A-T33A (T33A), Spy1A-S22A (S22A) or Spy1-S247A (S247A). (A) Cell lysates were

treated with nocadazole (G2 population; left panels) or untreated (Asynchronous population; right panel). Half of the population was kept for flow cytometry analysis (Fig. 5D). The remainder were lysed and immunoblotted with α-Myc for Spy1A (upper panels) and α-Actin (lower panels). (B) All samples were co-transfected with HA-Ub followed by treatment with MG132 for 14 hrs. Lysates were immunoprecipitated with α-Myc and immunoblotted for α-HA (upper panel) or α-Myc (lower panel). (C) 16 hrs. after transfection cyclohexamide was added, cells were collected at 30, 75 and 120 min. time points. Cell lysates were immunoblotted with α-Myc. Actin was used as a loading control (lower panel). Spy1 bands were quantified using densitometry and values corrected for using Actin. Relative densitometry over 3 separate experiments (right hand panel). Error bars represent SEM. Statistical data reflects comparisions between the wt transfected and mutant transfected cells at each time point. ** = $p<0.01$ (D) 293 cells were transfected with Myc-Spy1A-PCS3 (wt) or the triple mutant Spy1A-TST. 16 hrs post-transfection cells were treated with nocodazole and MG132 for 14 hrs. followed by orthophosphoric acid ^{32}P for an additional 4 hrs. Cells were lysed, immunoprecipitated with α-Myc and imaged on a Cyclone phosphorimager (upper blot). Immunoblot for α-Myc was used as a control (lower blot). Incorporation of ortho-phosphate was quantified using OptiQuant software, right panel represents results of one representative experiment of 2. (E) Cells from (A) were analyzed by flow cytometry. CPX analysis was carried out to determine the % of cells in each population and are depicted above the schematic of the cell cycle profiles. (F) Alive and dead cells were counted at 36 hrs. post-transfection using trypan blue exclusion. Error bars reflect standard deviation between 3 separate transfections and a standard T-test was performed assuming equal variance. Statistical data shown reflects comparisons between the wt transfected cells and mutant transfected cells * $p\leq 0.05$, ** $p\leq 0.01$.

Figure 1

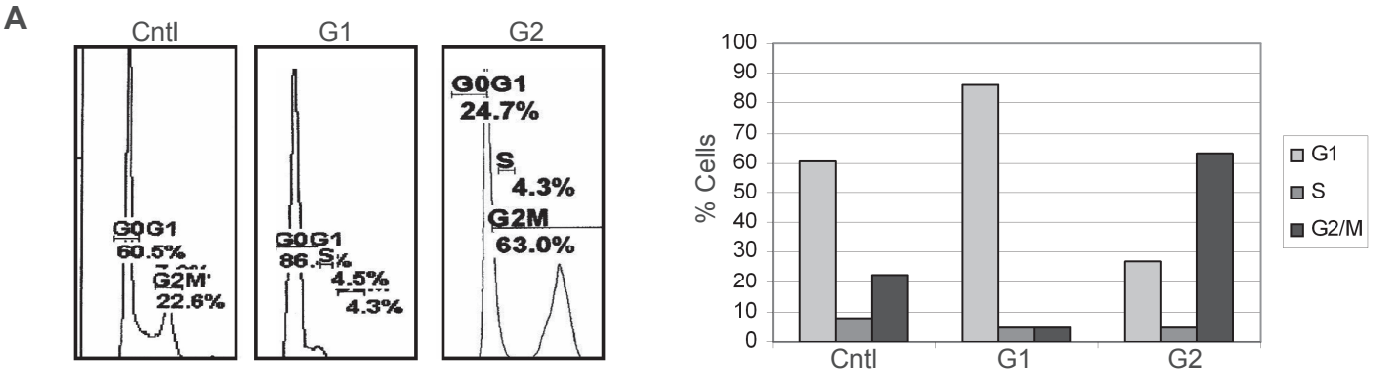

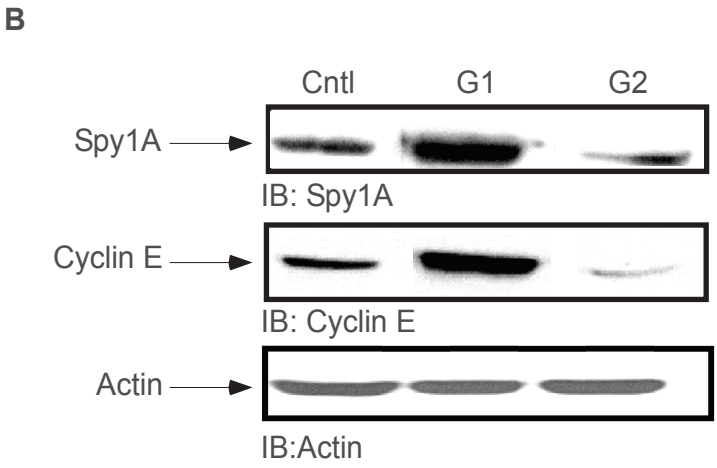

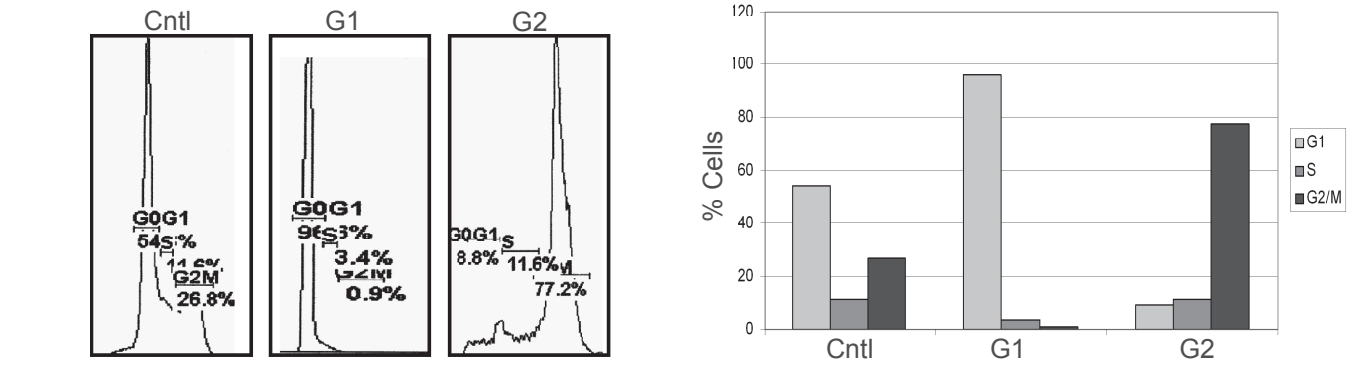

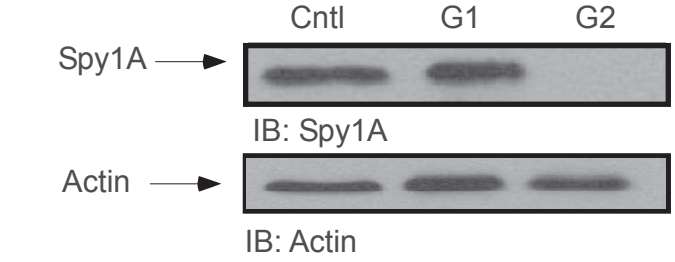

A

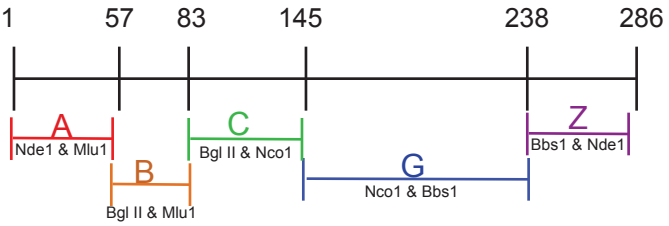

B

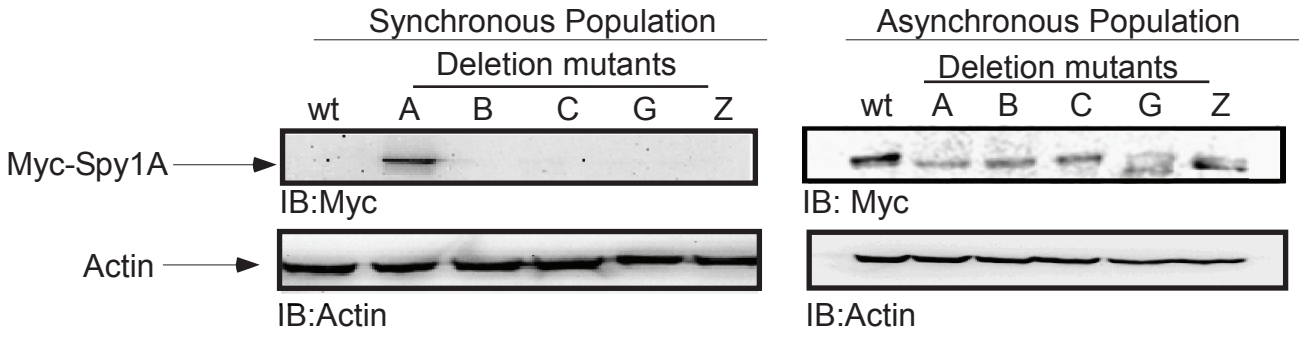

C

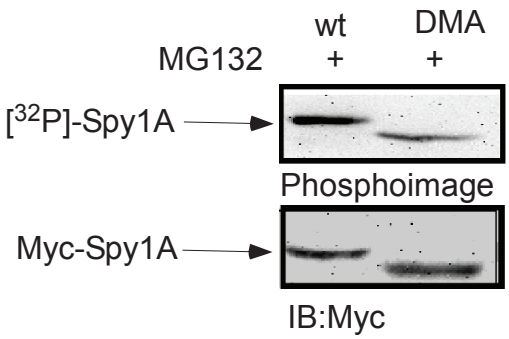

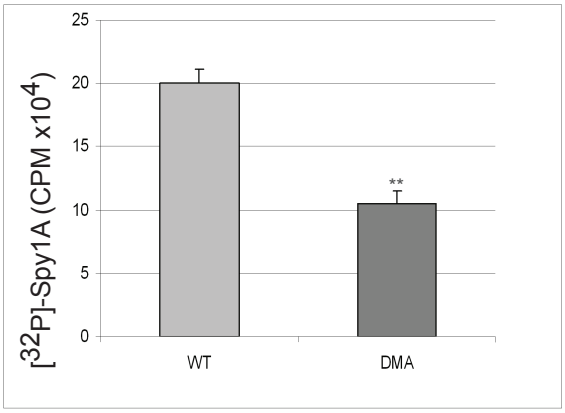

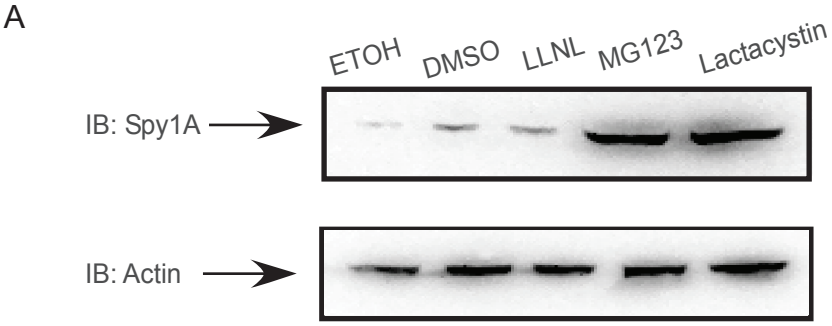

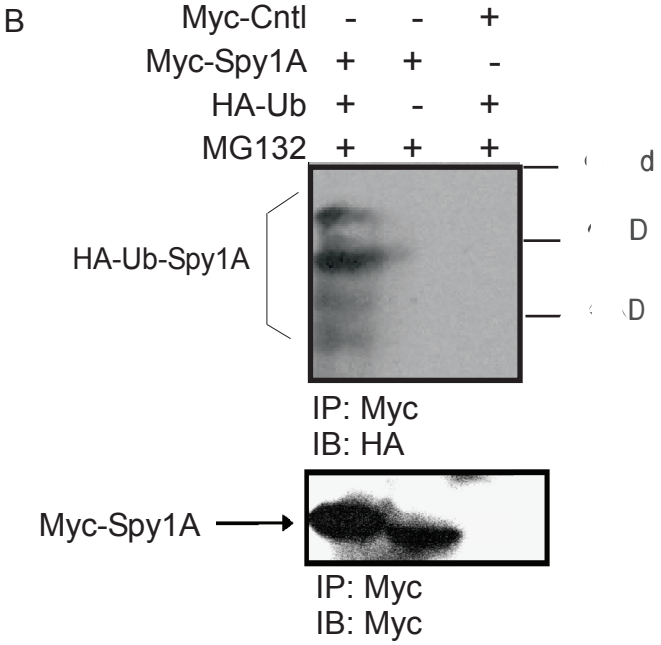

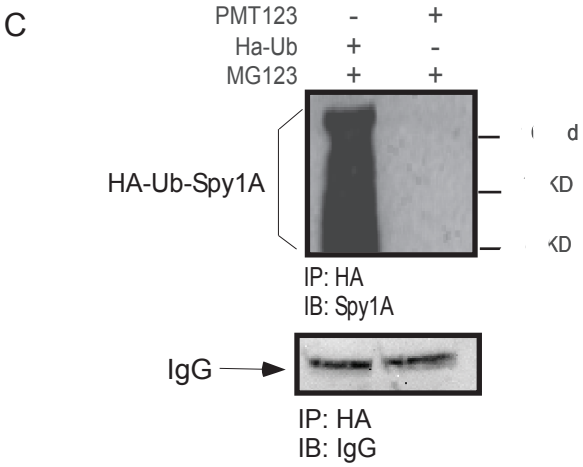

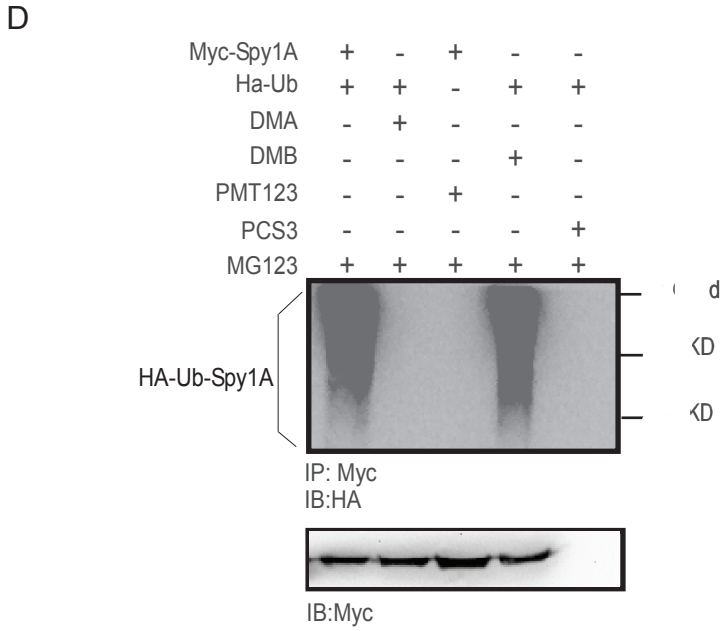

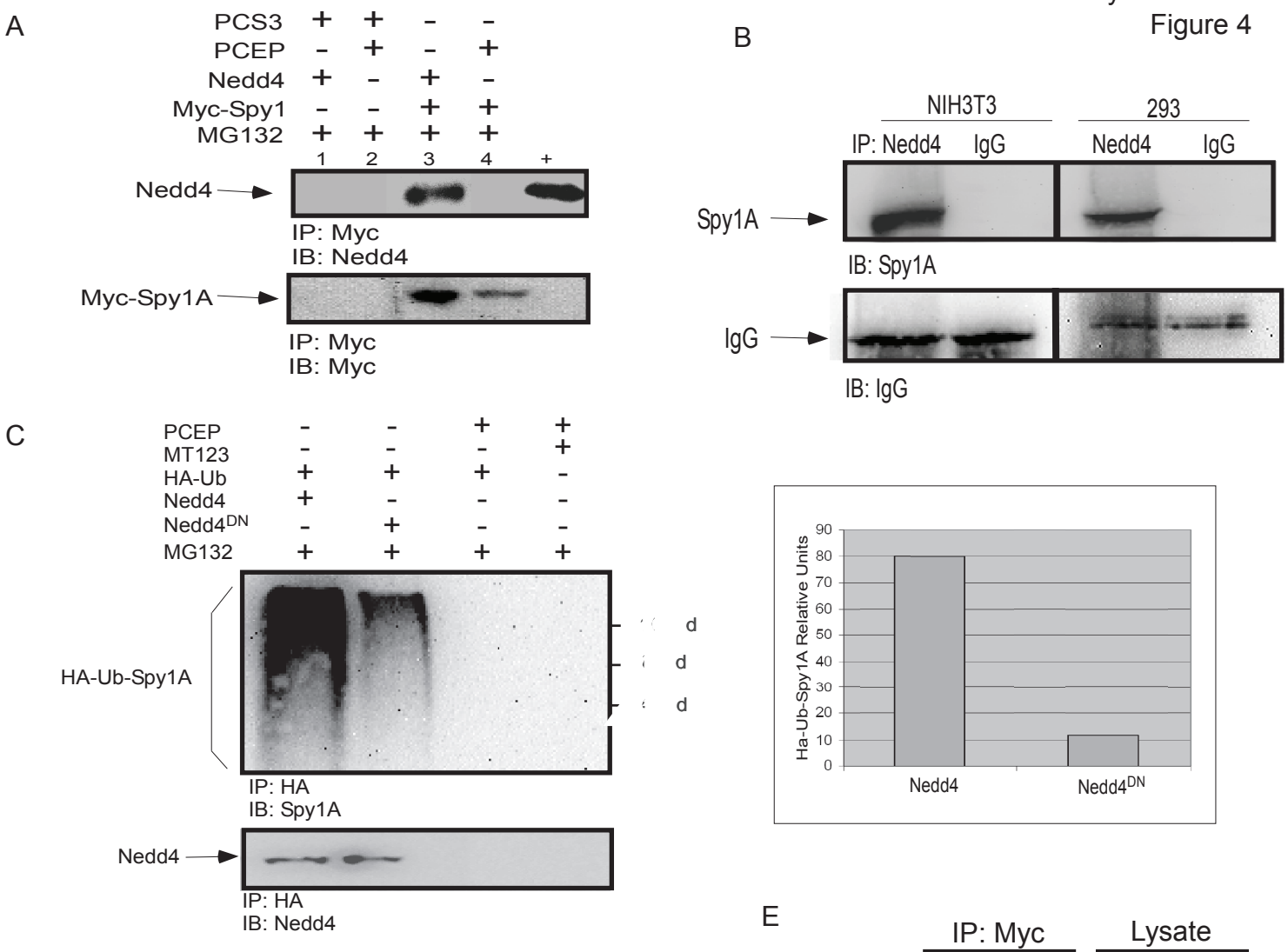

G

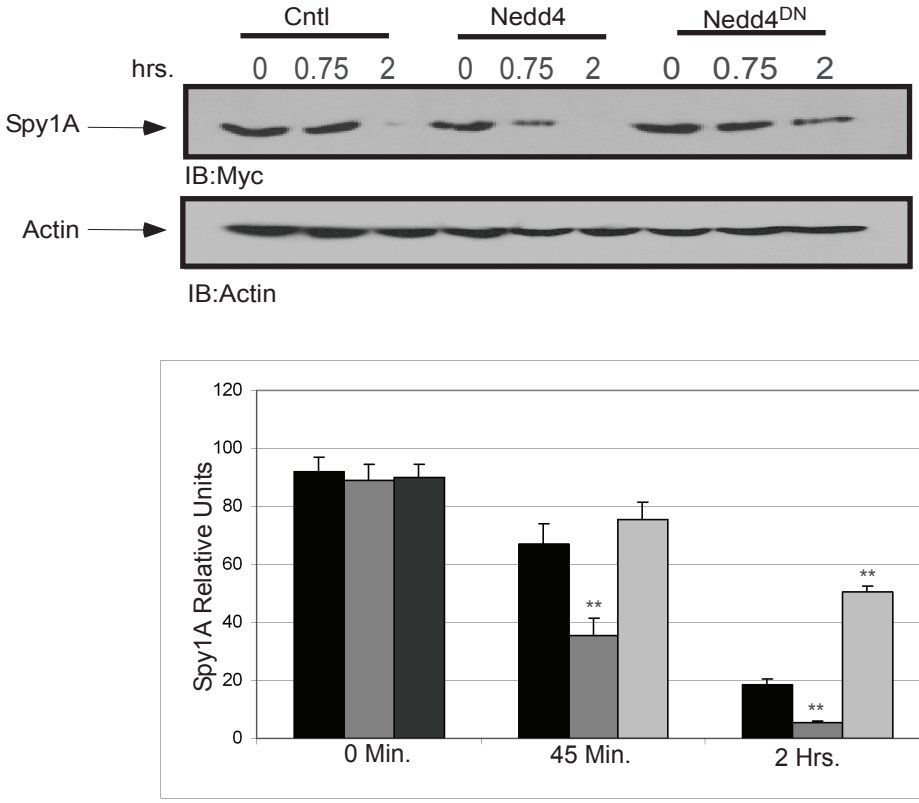

H